Supplement of Hydrol. Earth Syst. Sci., 29, 3745–3769, 2025
https://doi.org/10.5194/hess-29-3745-2025-supplement

Hydrology and Earth System Sciences
Open Access

Supplement of

Two-dimensional differential form of distributed Xinanjiang model

Jianfei Zhao et al.

Correspondence to: Zhongmin Liang (zmliang@hhu.edu.cn)

Section S1: Cross-sectional generalization and hydraulic parameters of river channel

In the two-dimensional differential-form of distributed Xinanjiang model (TDD-XAJ), the cross-section of river channel is generalized into a trapezoid (Fig. S1). Thus, the formulas for cross-sectional area, water surface width, and channel wetted perimeter could be given as:

$$A=\begin{cases}\varsigma h_{\mathrm{c}}+h_{\mathrm{c}}{}^{2}/\tan\beta & 0<\beta<90^{\circ}\\ \varsigma h_{\mathrm{c}} & \beta=90^{\circ}\end{cases}, \tag{S1}$$

$$B=\begin{cases}\varsigma+2h_{\mathrm{c}}/\tan\beta & 0<\beta<90^{\circ}\\ \varsigma & \beta=90^{\circ}\end{cases}, \tag{S2}$$

$$\chi=\begin{cases}\varsigma+2h_{\mathrm{c}}/\sin\beta & 0<\beta<90^{\circ}\\ \varsigma+2h_{\mathrm{c}} & \beta=90^{\circ}\end{cases}, \tag{S3}$$

where A is cross-sectional area (m^2), B is water surface width (m), χ is channel wetted perimeter (m), ς is channel bottom width (m), h_{c} is channel water depth (m), β is river bank slope gradient (°).

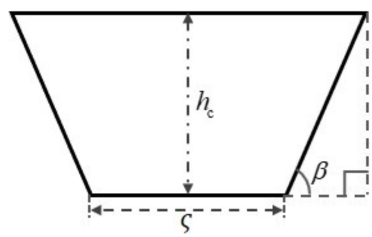

Figure S1. Diagram of trapezoidal cross-sectional generalization of river channel.

Section S2: The determination methods of spatially distributed model parameter

To determine spatially distributed model parameters, the process is generally based on spatially quantified data of watershed physical characteristics. This work is primarily carried out in two ways:

(1) **Lookup table-based method**. Parameters are determined from tables based on watershed physical attributes. Specifically, the ratio of the impervious area (A_{imp}) and coefficient of deep soil layer evapotranspiration (c) are determined according to land use types (Yao et al., 2012), while the determination of tension water storage capacity curve exponent (b) and free water storage capacity curve exponent (ex) are assigned based on soil types. The value of surface roughness coefficient (n_{s}) is assigned based on the land use type of each grid cell, with different land uses corresponding to different roughness coefficients, which are derived from existing literature (Miao et al., 2016; Perrini et al., 2024). For channel roughness coefficient (n_{c}), values are obtained from a roughness coefficient table for river channels (Arcement and Schneider, 1989).

(2) **Physical meaning-based method**. Parameter values are calculated using quantitative watershed physical characteristics according to the physical meaning of the parameters. Specifically:

a. Tension water storage capacity of the upper, lower, and deep soil layer (W_{um}, W_{lm}, and W_{dm}). The summation of W_{um}, W_{lm}, and W_{dm} represents the tension water capacity of the entire soil layer (W_{m}), and it can be determined according to soil hydrological parameters and soil layer depth (Yao et al., 2012), which could be expressed as:

$$W_{\mathrm{m}} = (\theta_{\mathrm{f}} - \theta_{\mathrm{r}})D_{\mathrm{s}}, \tag{S4}$$

where θ_{f} is field capacity, θ_{r} is residual water content, D_{s} is soil layer depth (mm). Subsequently, two watershed-scale uniform coefficients (K_{um} and K_{lm}) and their derived value $(1 - K_{\mathrm{um}} - K_{\mathrm{lm}})$ are used to divide W_{m} into W_{um}, W_{lm}, and W_{dm} accordingly, which are given as:

$$W_{\mathrm{um}} = W_{\mathrm{m}}K_{\mathrm{um}}, \tag{S5}$$

$$W_{\mathrm{lm}} = W_{\mathrm{m}}K_{\mathrm{lm}}, \tag{S6}$$

$$W_{\mathrm{dm}} = W_{\mathrm{m}}(1 - K_{\mathrm{um}} - K_{\mathrm{lm}}). \tag{S7}$$

b. Free water storage capacity (S_{m}). S_{m} usually represents the capacity of free water in the humus layer. Thus, it can be determined according to soil hydrological parameters and the humus layer depth (Yao et al., 2012), which could be expressed as:

$$S_{\mathrm{m}} = (\theta_{\mathrm{s}} - \theta_{\mathrm{f}})D_{\mathrm{h}}, \tag{S8}$$

where θ_{s} is saturated water content, θ_{f} is field capacity, D_{h} is humus layer depth (mm).

c. Interflow and groundwater outflow coefficient (K_{i} and K_{g}). K_{i} and K_{g} represent the outflow rate of interflow and groundwater. The method for determining K_{i} and K_{g} involves converting the free water storage to corresponding saturated water depth, based on the hillslope storage-discharge theory and steady-state assumptions, which is then multiplied by the slope gradient and saturated hydraulic conductivity using the kinematic wave assumption (Tong, 2022). K_{i} and K_{g} are finally expressed as the ratios of corresponding flow distance in the time interval of input forces to the slope length, which could be given as:

$$K_{\mathrm{i}} = \frac{2S_0 K_{\mathrm{su}} S_{\mathrm{hill}} \Delta T}{1000(\theta_{\mathrm{s}} - \theta_{\mathrm{f}})L_{\mathrm{hill}}^2}, \tag{S9}$$

$$K_{\mathrm{g}} = \frac{2S_0 K_{\mathrm{sl}} S_{\mathrm{hill}} \Delta T}{1000(\theta_{\mathrm{s}} - \theta_{\mathrm{f}})L_{\mathrm{hill}}^2}, \tag{S10}$$

where S_0 is free water storage (mm), K_{su} and K_{sl} is saturated hydraulic conductivity of the upper (representing interflow) and lower (representing groundwater) soil layer respectively (m s^{-1}), S_{hill} is the gradient of the slope, ΔT is the time interval of input forces (s), and L_{hill} is the length of the slope (m).

d. Interflow and groundwater storage recession coefficient (C_{i} and C_{g}). C_{i} and C_{g} represent the time delay for interflow and groundwater runoff as they travel from specific locations on the slope to the river channel. These parameters are determined based on the theory of spatially distributed unit hydrograph (Maidment et al., 1996; Tong, 2022). The grid cells that form the flow path extending from specific locations on the slope to the river channel is first identified using GIS. Then, using the kinematic wave assumption, the flow velocity of interflow and groundwater runoff through each grid cell is computed based on the saturated hydraulic conductivity of the upper and lower layers and the slope gradient. Finally, the time taken for flow through each grid cell is accumulated, which could be expressed as:

$$T_{\mathrm{i}} = \sum_{\mathrm{j}=1}^{N_{\mathrm{hill}}} L_{\mathrm{hill}}^{\mathrm{j}} / \left(K_{\mathrm{su}}^{\mathrm{j}} S_{\mathrm{hill}}^{\mathrm{j}}\right), \tag{S11}$$

$$T_{\mathrm{g}} = \sum_{\mathrm{j}=1}^{N_{\mathrm{hill}}} L_{\mathrm{hill}}^{\mathrm{j}} / \left(K_{\mathrm{sl}}^{\mathrm{j}} S_{\mathrm{hill}}^{\mathrm{j}}\right), \tag{S12}$$

where T_{i} and T_{g} is the accumulated travel time from specific locations on the slope to the river channel through interflow and groundwater respectively (s), N_{hill} is the count of grid cells that form the flow path. C_{i} and C_{g} for each grid cell are further derived using theoretical conversion, which could be given as:

$$C_{\mathrm{i}} = \exp(-\Delta T / T_{\mathrm{i}}), \tag{S13}$$

$$C_{\mathrm{g}} = \exp\left(-\Delta T / T_{\mathrm{g}}\right). \tag{S14}$$

The primary data used to determine spatially distributed model parameters include soil physical and hydraulic properties, slope gradient, and land use. These can be obtained from open-source datasets, such as Harmonized World Soil Database v2.0 (HWSD v2.0) (FAO and IIASA, 2023), China dataset of soil properties for land surface modelling version 2 (CSDLv2) (Shi et al., 2025), and Global land cover mapping at 30m resolution (GlobeLand30) (Chen et al., 2015).

Table S1: Nomenclature

Symbol	Signification	Unit
A	Cross-sectional area	m^2
A_{c}	Open water surface area of the channel control volume	m^2
A_{imp}	The ratio of the impervious area	-
b	The exponent of tension water storage capacity curve (TWSCC)	-
B	Water surface width	m
c	Coefficient of deep soil layer evapotranspiration	-
C_{g}	Groundwater storage recession coefficient	-
C_{i}	Interflow storage recession coefficient	-
ex	The exponent of free water storage capacity curve (FWSCC)	-
E_{d}	Actual evapotranspiration intensity from the deep soil layer	mm s^{-1}
E_{l}	Actual evapotranspiration intensity from the lower soil layer	mm s^{-1}
E_{n}	Net evapotranspiration intensity	mm s^{-1}
E_{obs}	Pan evaporation intensity	mm s^{-1}
E_{u}	Actual evapotranspiration intensity from the upper soil layer	mm s^{-1}
f_{w}	Runoff coefficient or the ratio of areas where tension water capacity is satisfied	-
F_{i}	Interflow intensity in external normal vector direction at boundary of slope control volume	mm s^{-1}
g	Acceleration due to gravity	m s^{-2}
h_{c}	Channel water depth	m
$h_{\mathrm{c,eff}}$	Effective water depth at the boundary of channel control volume	m
h_{s}	Surface water depth	m
$h_{\mathrm{s,eff}}$	Effective water depth at the boundary of slope control volume	m

Symbol	Signification	Unit
i	Index of slope control volume in x direction or index of the channel control volume	-
I_l	Recharge intensity from the lower to deep soil layer	mm s^{-1}
I_u	Recharge intensity from the upper to lower soil layer	mm s^{-1}
j	Index of slope control volume in y direction	-
K_e	Coefficient of potential evapotranspiration to pan evaporation	-
K_g	Groundwater outflow coefficient	-
K_i	Interflow outflow coefficient	-
n	The length of the simulated or observed discharge sequence	-
n_c	Channel roughness coefficient	s $m^{-1/3}$
n_s	Surface roughness coefficient	s $m^{-1/3}$
O_g	Groundwater storage	mm
O_i	Interflow storage	mm
P	Total amount of precipitation	mm
P_n	Net precipitation intensity	mm s^{-1}
P_{obs}	Observed precipitation intensity	mm s^{-1}
Q_c	Channel discharge in external normal vector direction at boundary of channel control volume	m^3 s^{-1}
$Q_{c,up}$	Summation of Q_c from multiple upstream channel segments	m^3 s^{-1}
Q_g	Outflow intensity of the groundwater storage	mm s^{-1}
$Q_{g,up}$	Summation of Q_g from multiple upstream grids	mm s^{-1}
Q_i	Outflow intensity of the interflow storage	mm s^{-1}
$Q_{i,up}$	Summation of Q_i from multiple upstream grids	mm s^{-1}
$Q_{i,x}$	The x-directional components of Q_i	mm s^{-1}
$Q_{i,y}$	The y-directional components of Q_i	mm s^{-1}
Q_{obs}	Observed discharge	m^3 s^{-1}
Q_{sc}	Exchange discharge between the slope surface and the channel	m^3 s^{-1}
Q_{sim}	Simulated discharge	m^3 s^{-1}
Q_{ZDG}	Outflow discharge at the watershed outlet using zero-depth gradient (ZDG) condition	m^3 s^{-1}
R	Total runoff intensity	mm s^{-1}
R_g	Groundwater intensity	mm s^{-1}
R_i	Interflow intensity	mm s^{-1}
R_{ps}	Surface runoff intensity from the pervious areas	mm s^{-1}
R_s	Total surface runoff intensity	mm s^{-1}
S_{fc}	Channel friction term	-
S_{fx}	Surface friction term in x direction	-
S_{fy}	Surface friction term in y direction	-
S_m	Free water storage capacity	mm
S_{mm}	Maximum single-point free water storage capacity	mm
S_0	Free water storage	mm
S_{oc}	Channel bottom slope term	-
S_{ox}	Surface bottom slope term in x direction	-
S_{oy}	Surface bottom slope term in y direction	-
t	Time	s
T	Total simulation time	s
u	Surface flow velocity in x direction	m s^{-1}
v	Surface flow velocity in y direction	m s^{-1}

Symbol	Signification	Unit
w	Channel flow velocity	m s^{-1}
W_{d}	Tension water storage of the deep soil layer	mm
W_{dm}	Tension water storage capacity of the deep soil layer	mm
W_{l}	Tension water storage of the lower soil layer	mm
W_{lm}	Tension water storage capacity of the lower soil layer	mm
W_{mm}	Maximum single-point tension water storage capacity	mm
W_{u}	Tension water storage of the upper soil layer	mm
W_{um}	Tension water storage capacity of the upper soil layer	mm
z_{bank}	Channel bank elevation	m
z_{c}	Channel bottom elevation	m
z_{s}	Surface elevation	m
α	Courant-Friedrichs-Lewy (CFL) condition coefficient	-
β	River bank slope gradient	°
γ	Slope aspect	°
Γ	The boundary of control volume	-
δl	Distance between two neighboring grid centers	m
Δl	Channel segment length	m
Δt	Model time step	s
Δt_{max}	Maximum model time step without further user-defined or programmatic constrain	s
ΔT	Time interval of input forces	s
Δx	Grid size	m
ε_{g}	Ratio of groundwater outflow intensity from slope to channel	-
ε_{i}	Ratio of interflow outflow intensity from slope to channel	-
η_{c}	Water surface elevation in channel	m
η_{s}	Water surface elevation on slope surface	m
ς	Channel bottom width	m
ϕ_{c}	Source term of channel	m s^{-1}
ϕ_{g}	Source term of groundwater storage	mm s^{-1}
ϕ_{i}	Source term of interflow storage	mm s^{-1}
ϕ_{s}	Source term of surface	m s^{-1}
χ	Channel wetted perimeter	m
Ω	Control volume	-

References

Arcement, G. J. and Schneider, V. R.: Guide for selecting Manning's roughness coefficients for natural channels and flood plains, 2339, https://doi.org/10.3133/wsp2339, 1989.

Chen, J., Chen, J., Liao, A., Cao, X., Chen, L., Chen, X., He, C., Han, G., Peng, S., Lu, M., Zhang, W., Tong, X., and Mills, J.: Global land cover mapping at 30m resolution: A POK-based operational approach, ISPRS-J. Photogramm. Remote Sens., 103, 7-27, https://doi.org/10.1016/j.isprsjprs.2014.09.002, 2015.

FAO and IIASA: Harmonized world soil database (version 2.0) [dataset], https://www.fao.org/soils-portal/data-hub/soil-maps-and-databases/harmonized-world-soil-database-v20/en/, 2023.

Maidment, D. R., Olivera, F., Calver, A., Eatherall, A., and Fraczek, W.: Unit hydrograph derived from a spatially distributed velocity field, Hydrol. Process., 10, 831-844, https://doi.org/10.1002/(SICI)1099-1085(199606)10:6<831::AID-HYP374>3.0.CO;2-N, 1996.

Miao, Q., Yang, D., Yang, H., and Li, Z.: Establishing a rainfall threshold for flash flood warnings in China’s mountainous areas based on a distributed hydrological model, J. Hydrol., 541, 371-386, https://doi.org/10.1016/j.jhydrol.2016.04.054, 2016.

Perrini, P., Cea, L., Chiaravalloti, F., Gabriele, S., Manfreda, S., Fiorentino, M., Gioia, A., and Iacobellis, V.: A runoff-on-grid approach to embed hydrological processes in shallow water models, Water Resour. Res., 60, e2023WR036421, https://doi.org/10.1029/2023WR036421, 2024.

Shi, G., Sun, W., Shangguan, W., Wei, Z., Yuan, H., Li, L., Sun, X., Zhang, Y., Liang, H., Li, D., Huang, F., Li, Q., and Dai, Y.: A china dataset of soil properties for land surface modelling (version 2, csdlv2), Earth Syst. Sci. Data, 17, 517-543, https://doi.org/10.5194/essd-17-517-2025, 2025.

Tong, B.: Fine-scale rainfall-runoff processes simulation using grid Xinanjiang (grid-XAJ) model, Hohai University, Nanjing, Jiangsu, 2022.

Yao, C., Li, Z., Yu, Z., and Zhang, K.: A priori parameter estimates for a distributed, grid-based Xinanjiang model using geographically based information, J. Hydrol., 468-469, 47-62, https://doi.org/10.1016/j.jhydrol.2012.08.025, 2012.